Renewable and Sustainable Energy Reviews 149 (2021) 111387

Contents lists available at ScienceDirect

Renewable and Sustainable Energy Reviews

journal homepage: www.elsevier.com/locate/rser

Liquid metal battery storage in an offshore wind turbine: Concept and economic analysis

J.G. Simpson [a,*], G. Hanrahan [a], E. Loth [a], G.M. Koenig [b], D.R. Sadoway [c]

[a] Department of Mechanical and Aerospace Engineering, University of Virginia, 122 Engineer's Way, Charlottesville, VA, 22903, USA
[b] Department of Chemical Engineering, University of Virginia, 102 Engineer's Way, Charlottesville, VA, 22904, USA
[c] Department of Materials Science and Engineering, Massachusetts Institute of Technology, 77 Massachusetts Avenue, Cambridge, MA, 02139, USA

A R T I C L E I N F O

Keywords:
Wind energy
Energy storage
Liquid metal battery
Li-ion
Energy arbitrage
Integration
Levelized cost of energy (LCOE)
Cost

A B S T R A C T

As wind energy increases its global share of the electrical grid, the intermittency of wind becomes more problematic. To address the resulting mismatch between wind generation and grid demand, long-duration (day-long) low-cost energy storage is offered as a potential solution. Lithium-ion (Li-ion) storage is an obvious, well-developed candidate, but it is currently too expensive for such long-duration applications. Liquid metal battery (LMB) storage offers large cost reductions and recent technology developments indicate it may be viable for MW-scale storage. Accordingly, we investigate co-locating and integrating LMB and Li-ion storage within the substructure of an offshore wind turbine. Integration allows the substructure to cost-effectively double as a storage container and allows for costly electrical farm-to-shore connections to be reduced to near the average power size (by reducing peak power). These benefits are compared to the costs for battery integration. Simulations show that line size can be reduced by 20% with 4 h of storage or by 40% with 12 h of storage, with negligible capacity factor losses. However, with 24 h of average power storage using LMB, no line size reduction provided the best overall net value of the turbine-storage system due to the ability to capture all available wind energy and profit from energy arbitrage and full capacity credit. In general, LMB integrated storage results in an increased relative value with current system costs. Projected technology trends indicate that these benefits will significantly improve and that integrated Li-ion storage will also become cost-effective.

1. Introduction

Wind energy already provides more than a quarter of the electricity consumption in three countries around the world [1], and its share of the energy grid is expected to grow as offshore wind technology matures. The wind speeds on offshore projects are much steadier and faster than wind speeds on land, and offshore wind provides a location that is close to high demand coastal areas and avoids space constraints [2].

However, as grid penetration from variable (inconstant) renewable sources increases worldwide, their intermittency becomes more problematic [3]. As seen in Fig. 1, wind generation does not align well with times of electricity demand. Furthermore, the relative value of wind energy decreases when it becomes a larger fraction of the grid generation [4,5]. When in demand, renewable energy sources may have a high value compared to baseload generation, e.g., such as when solar produces power during the day at times of relatively high demand. However, the value of these resources falls when a glut of renewable energy with no marginal cost enters the market and depresses prices or forces curtailment of renewable resources [4,6]. This issue is expected to intensify since the electrical market structure is moving away from a purely energy-based market and towards a structure with greater focus on capacity and grid services [7]. While some have suggested improving forecasting methods to better handle renewable energy on the grid [8], another potential way to deal with these issues is to install high-capacity energy storage that can shift the time of generation to times when demand is stronger [9]. This will require a low-cost energy storage solution that can provide storage for hours or even days. In this future, renewable energy could increase its value significantly by pairing with storage systems, allowing it to participate in capacity markets, energy arbitrage, and auxiliary services.

Multiple strategies have been pursued to optimize the operation of battery storage with variable renewable energy. These include reducing the error between the forecasted wind power and the actual wind power [10,11], using a combination of energy storage and demand-side management [12], introducing incentives [13], and using large-scale

* Corresponding author.
E-mail address: js9sw@virginia.edu (J.G. Simpson).

https://doi.org/10.1016/j.rser.2021.111387
Received 21 April 2020; Received in revised form 1 June 2021; Accepted 20 June 2021
Available online 30 June 2021
1364-0321/

Nomenclature

Symbols

C	Battery C rate [1/hrs]
G	Energy generated [MW]
k	Heat transfer coefficient [W/m-k]
P	Power [MW]
q	Heat rate [kW]
r	Radius [m]
t	Thickness [cm]
T	Temperature [°C]
V	Battery volume [m^3]
W	Wind speed [m/s]
η	Charge or discharge efficiency [%]

Subscripts

avg	Average power
b	Battery
heater	Heater
i	Insulation
Joule	Joule heating
loss	Heat loss
rated	Rated power
storage	Storage system
total	Combined system
turbine	Wind turbine system
w	Water
wall	Substructure wall

Abbreviations

AEP	Annual energy production [MWh/yr]
BOS	Balance of station
CapEx	Capital expenses [$]
CC	Capacity credit [%]
CF	Capacity factor [%]
CP	Capacity payment [$/yr]
CV	Capacity value [$/MW-day]
FCR	Fixed charge rate [1/yr]
LACE	Levelized avoided cost of energy [$/MWh]
LCOE	Levelized cost of energy [$/MWh]
Li–Bi	Li | LiCl–LiBr–LiI | Bi battery chemistry
Li-ion	Lithium-ion
LMB	Liquid metal battery
MGP	Marginal generation price [$/MWh]
NV	Net value [$/MWh]
OpEx	Operating expenses [$/yr]
SCAPP	Storage capacity at average plant power [hrs]
SCRPP	Storage capacity at rated plant power [hrs]
VSD	Variable speed drive

transmission systems [14] to integrate high shares of wind energy.

One potential advantage to storage with wind energy is the ability to employ time-shifting for energy arbitrage. Previous work and modeling in energy arbitrage suggests that batteries are too expensive to break-even in most arbitrage markets [15–18]. Salles [17] simulated energy storage systems in PJM (a mid-Atlantic electrical transmission organization) over 2008 to 2014 and found the best possible scenario yielded enough revenue to breakeven with battery installed costs at $200/kWh; however, other locations, during other years, required installation costs of half that value to break even [17]. As such, the more likely potential advantages to storage with wind energy are to time-shift the energy generated, balance the grid, and provide additional peak reserves [3,9].

Battery storage system capacity is typically quantified based on nameplate duration of discharge, or how many hours the battery can discharge at full rated battery power generation. Battery storage capacity is thus specified as, short-duration: less than 0.5 h of rated capacity, medium-duration: 0.5–2 h of rated capacity, or long-duration: more than 2 h of rated capacity [19]. For grid applications, 4 h of rated capacity may be more representative of "long-duration" storage [20,21]. This is an appropriate and critical quantification of the battery; however, for a storage system co-located and integrated with a plant, it is important to also consider the battery storage capacity relative to the plant power.

Thus far, battery storage systems co-located with wind turbines are small relative to turbine power generation. GE installed a wind farm consisting of 13 turbines, with total rated generation of 37 MW for their Tullahennel project in north-western Ireland, where each turbine is accompanied by a Li-ion battery to provide a total of 897 kWh of storage [22]. Deepwater Wind recently won a bid from the state of Rhode Island to build a 144 MW wind farm co-located with a 10 MW/40 MWh Tesla battery, with a goal of shifting energy production to meet peak demand [23]. The largest battery storage system in the world is the Hornsdale

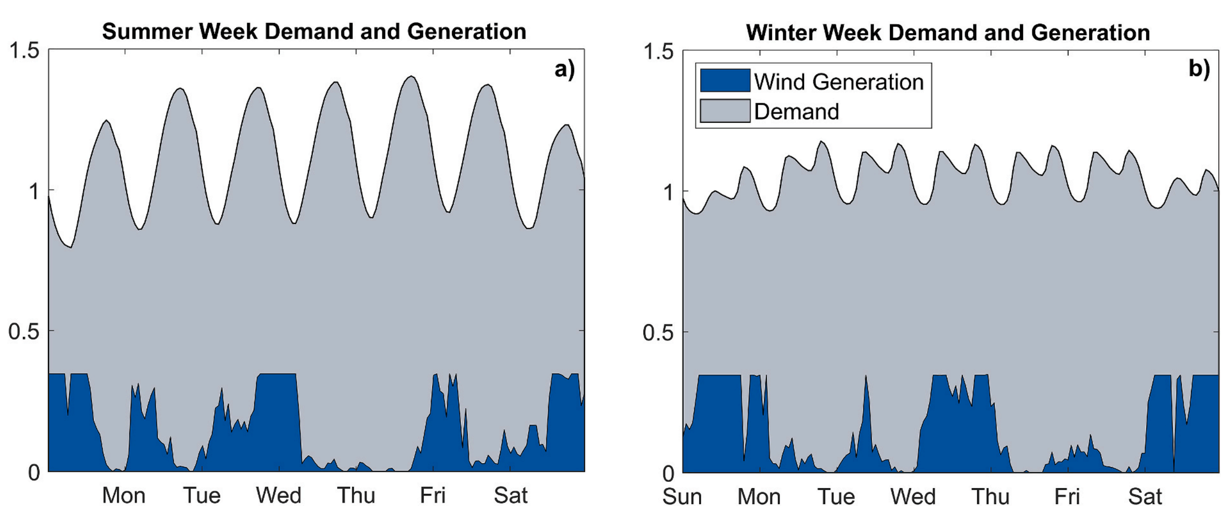

Fig. 1. Offshore wind energy generated at 15% penetration compared to electrical grid demand (both normalized by annual average) over a representative week for a) summer, and b) winter.

Power Reserve installed in South Australia in 2017; the system consists of 315 MW of wind power combined with a 100 MW/129 MWh battery used primarily for the purposes of grid stabilization [24].

If one considers the battery capacity relative to the plant power (not the rated battery power limit), these installations would all store an hour or less of average wind power. While such energy storage capacity has not been commonly defined nor reported (to the authors' knowledge), this characterization can value the integrated performance of a system composed of an energy source and its associated energy storage. This is important as wind energy can have periods of little or no generation that exceed 12 h as shown in Fig. 1. A power spectral density analysis in Ref. [25], found that using energy storage to help smooth out the most common frequencies of wind power oscillation (12-h and 24-h) will likely require long-duration storage. As such, substantial levelization and/or demand-shaping requires storage in the range of 10–24 h of average wind plant power [26]. Thus, if battery storage is going to be used to significantly levelize and control wind energy generation for day-to-day operation, then new storage options will be needed that are operable over much longer durations in the context of storage capacity relative to the plant average or rated power. In particular, none of the current or planned wind energy storage projects are able to address the majority of wind energy generation intermittency.

Therefore, there is significant interest in the potential benefits for energy storage systems that have the capacity to store a fraction of a day up to a full day or more of average power [27]. The solution would seem to indicate that more storage capacity is needed for a given wind farm. However, utility-scale energy storage for even day-long duration is currently prohibitively expensive with conventional battery technologies. Limited options for low-cost, high-performance energy storage are even inspiring hybrid energy storage systems instead [28].

As noted above, a key to employing long-duration energy storage for wind is to ensure that the capacity comes at low enough cost with respect to the benefits it can provide. The cost for electrical energy storage is often driven by materials, packaging, and level of development. Currently, the most commonly installed and well-developed electrical energy storage option is Li-ion batteries. Li-ion battery costs have dropped 85% from 2010 to 2018 [29], and battery pack prices have been projected to reach between \$62/kWh and \$76/kWh by 2030 [30]. Despite the declining prices, Li-ion batteries come with certain disadvantages, especially at MW-scale. They have a tendency to overheat, sometimes leading to thermal runaway and combustion [31,32]. Li-ion batteries also operate within a narrow temperature region and have significantly reduced performance outside that temperature region necessitating active thermal management systems [32]. Li-ion batteries can have a lifetime of more than 3500 cycles or 10 years operation with a wind farm, over which their capacity declines (since cycle life is nominally defined by 20% capacity loss) [33]. As such, integrated Li-ion batteries would need to be significantly oversized or replaced at least once during the 20–30 year life of a wind turbine to continue providing adequate storage capacity.

An alternative electrical storage option that has been developed in recent years and may be approaching commercial production is the liquid metal battery (LMB) [34–39]. These batteries feature low raw-material cost, high thermal resilience, and long lifespan, and thus are judged to be a good fit for large-scale energy storage [37]. Additionally, their chemistries are neither volatile nor flammable. The liquid metal electrodes and molten salt electrolyte must be operated at elevated temperature so as not to solidify. With proper insulation, LMB can maintain operating temperature by generating adequate heat while cycling (charging and discharging) without the need for auxiliary heaters [39]. This feature favors LMB for large-scale storage applications (MWh) rather than small-scale storage applications (kWh). This paper will focus on the working composition "Li | LiCl–LiF | Bi" as specified in Ref. [35] and herein referred to as "Li–Bi", where the anode is Lithium, the electrolyte is LiCl–LiF, and the cathode is Bismuth. This composition will be used because it has operational metrics reported in the literature. However, Ambri, a company working to commercialize the LMB technology, has recently announced a new Ca–Sb battery composition which is expected to exceed the high performance of Li–Bi while reducing the cost of storage even further to well below the projected price of Li-ion [39].

The significant benefits of long-duration storage for wind energy combined with recent developments in LMB technology suggest that this combination may have strong potential to address intermittency, especially offshore where storage can reduce farm-to-shore electrical connection costs. In order to investigate this hypothesis in a system-based cost-effective manner, the objectives of this work are: i) to develop a technical concept design for integrating LMB into a monopile offshore wind turbine to examine influence of storage capacity and electrical connection line size on overall capacity factor (Section 2), and ii) to determine the expected cost and value of such a wind-integrated battery system and compare these to those of a wind turbine with no energy storage and one with Li-ion battery storage (Section 3).

This is the first study, to the authors' knowledge, that investigates integration of wind turbines with LMB storage and the first to consider offshore energy storage capacity factors and economics for long-duration storage. This study is also the first to parameterize the battery capacity relative to the average plant power generation (not just the battery rated generation power). This capacity parameter represents a change in perspective which characterizes the energy storage and the energy source as an integrated system. As the LMB concept combined with a wind turbine has not been explored before in terms of an engineering nor a cost basis, the present work is based on a first-order analysis to evaluate the leading factors that govern performance and cost.

2. Concept design

2.1. Capacity at average plant power

As discussed above, energy storage capacity is typically measured based on the discharge time at rated power. This gives hours of storage capacity in terms of rated battery power, i.e. the time it takes to drain the battery at the maximum discharge rate. However, when thinking about integrating an energy storage system with a power plant (such as a wind farm), we can also measure the storage capacity in relation to the output power from the plant. This approach means that as the generation scales up or down, the associated storage hours can stay constant while the actual capacity (in MWh) varies. Quantifying the integrated storage capacity can either be defined relative to the rated (maximum) power of the plant or the average power produced by the plant, where the plant may be a solar farm, wind turbine, nuclear generator, etc. For these definitions, the rated and average power are proposed to be defined as that without storage to ensure a consistent baseline reference. In particular, for the rated version, we define storage capacity at rated plant power (SCRPP) in hours as the ratio of total storage capacity (MWh) to rated plant power (MW)

$$SCRPP = \frac{Total\ Storage\ Capacity\ (MWh)}{P_{rated}(MW)} \tag{1}$$

However, since the typical goal of co-located storage is to smooth or level the output from a variable renewable power plant, the average power production is more germane. For this, we define the storage capacity at average plant power (SCAPP) as the ratio of total storage capacity (MWh) to the mean (or average) wind power (MW) in hours and relate this to the plant capacity factor (CF)

$$SCAPP = \frac{Total\ Storage\ Capacity\ (MWh)}{P_{avg}(MW)} = \frac{Total\ Storage\ Capacity\ (MWh)}{P_{rated}(MW) \times CF} \tag{2a}$$

$$CF = \frac{P_{avg}}{P_{rated}} \tag{2b}$$

The latter expression uses the conventional definition of plant capacity factor as the average power (P_{avg}) normalized by the rated plant power (P_{rated}). A typical photovoltaic solar system will have a CF of about 15%–25% with predictable daily cycles while a typical wind turbine will have a CF of 30%–50% with more irregular day-to-day, week-to-week and even season-to-season variations. Thus, storing one or more days of energy at average power (e.g. SCAPP >24 h) is needed to achieve nearly levelized wind energy generation. However, there are significant benefits for partial levelization and as such a range of SCAPP durations will be considered to provide the best net economic value for the integrated system.

2.2. Overview of turbine for storage integration

We propose placing a battery storage system within the tower of an offshore wind turbine, as depicted in Fig. 2a. The integrated battery storage would allow the wind turbine system to regulate when and how much power it is producing and control what power travels along the electrical lines to shore. The battery would interact with the variable speed drive (VSD) as depicted in Fig. 2b, thereby removing the need for additional power electronics in the system [40,41]. Thus, DC power would travel along the turbine tower to and from the battery, while AC power would travel out of the VSD and through lines to shore.

One benefit of the proposed system is the possibility of reducing the size of the electrical lines to shore and the corresponding infrastructure. An example of how this storage system would function with reduced electrical line size is shown in Fig. 3 for a 5 MW turbine with a 2.5 MW line size and 6 h of storage at average turbine power, i.e. 6 h of SCAPP. When more wind power is generated than the maximum power that the transmission line can handle, the excess power charges the battery until it is full, and then the excess power is curtailed. When less wind power is produced than the line size, the battery discharges to provide additional power. This scheme attempts to provide power at a constant level as often as possible, but other storage schemes could seek to maximize energy revenue or to smooth the hour-to-hour output of wind energy, all of which will have different costs and values.

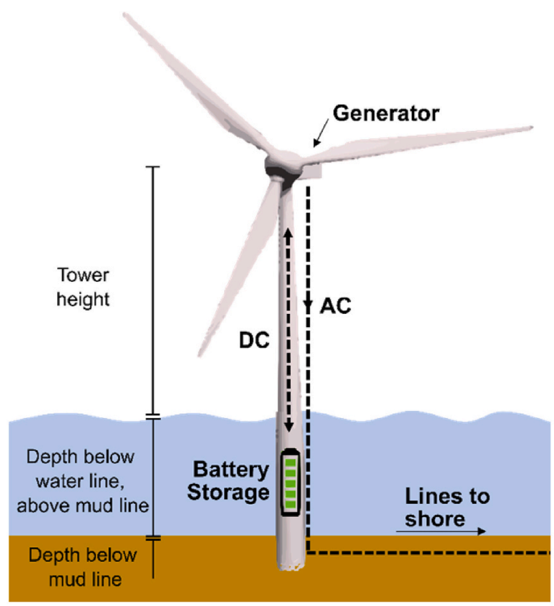

a

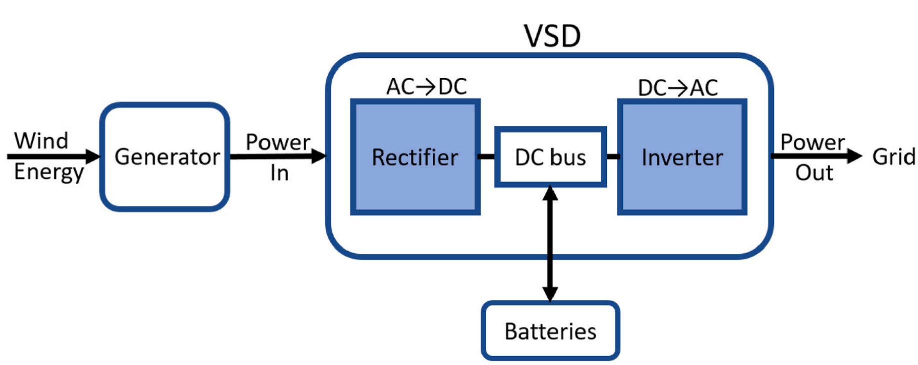

b

Fig. 2. a. Battery storage integrated into offshore wind turbine tower. Tower and substructure heights are denoted on the left and are specified for the NREL 5 MW turbine in Table 1. Fig. 2b. Battery connection to wind turbine electrical system via variable speed drive (VSD) [41].

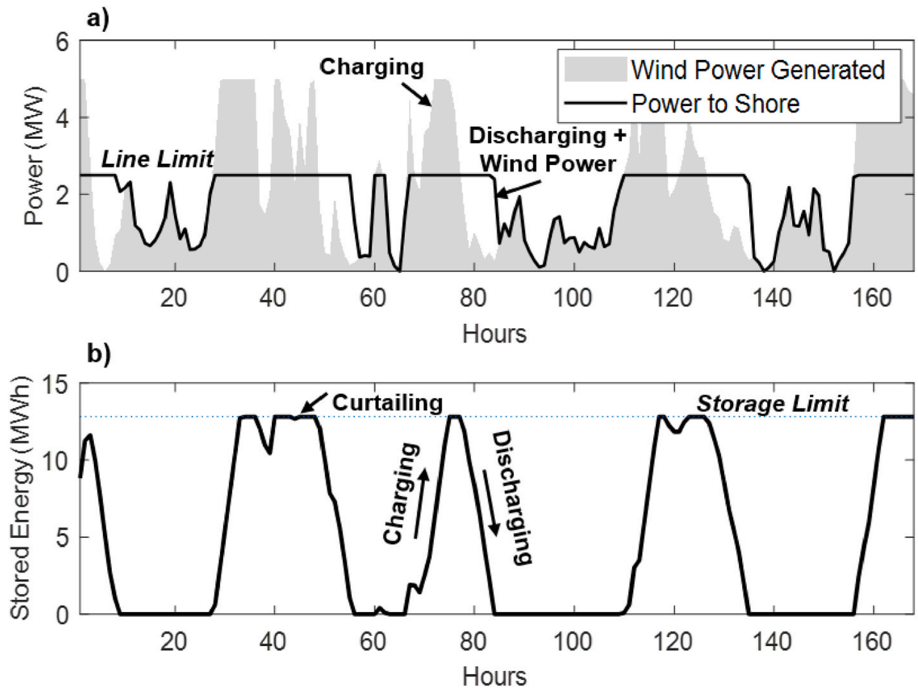

Fig. 3. Energy storage example for a 5 MW turbine over one week with a 2.5 MW electrical line size and 6 h of SCAPP, where times of charging, discharging, and curtailing are highlighted for a) power generated from the rotor and power sent to shore, as well as b) energy stored in the battery.

Wind speed data were gathered from the DOE BUOY project during its deployment off the coast of Virginia at a height of 90 m [42]. A representative week of hourly wind speed data was pulled from the DOE BUOY data (a week with typical periods of high and low wind speeds and no missing data points) and was used throughout this paper. The probability distribution of the one week of data used herein and the entire year of data are shown in Fig. 4, with a Weibull distribution fitted to the year of wind speed data described by $Scale = 9.5$ and $Shape = 2.1$. Using one week of data reduced computational time while still capturing the important time scales on which the proposed storage system would be operating.

The energy production of the wind turbine is based on values from the NREL 2017 Cost of Wind Energy Review [45] to allow for direct comparison with the LCOE breakdown provided in that report. The week of wind speed data was converted to wind power data using Eq. (3) by applying the NREL 5 MW reference turbine power coefficient curve [43] and scaling the wind speeds such that the average wind power yielded a capacity factor of 0.427 to be consistent with the 2017 Cost of Wind Energy Review [45]. For the baseline conventional 5 MW turbine (without storage and with the original electrical connection line size of 5 MW), resulting wind power generated (G) as a function of wind speed (W) is then given by

$$W < 3m/s \text{ or } W > 25\ m/s \quad G = 0\ MW \tag{3a}$$

$$3m/s \leq W < 11.4\ m/s \quad G = 0.00343 \times W^3\ MW \tag{3b}$$

$$11.4m/s \leq W \leq 25\ m/s \quad G = 5MW \tag{3c}$$

For simplicity, wind farm wake losses and dynamic effects of turbulence are ignored when converting wind speed data into wind power results, as is typical in initial designs.

For this conceptual design of integrated storage, the baseline wind turbine was the monopile offshore NREL 5 MW reference turbine [43], whose details are given in Table 1. The turbine tower and substructure heights are denoted in Fig. 2a. The battery system can be integrated into the monopile substructure of the turbine, either above water or below water, to create an integrated wind-storage system. The batteries will be considered with long-duration options of 6, 12, and 24 h of SCAPP,

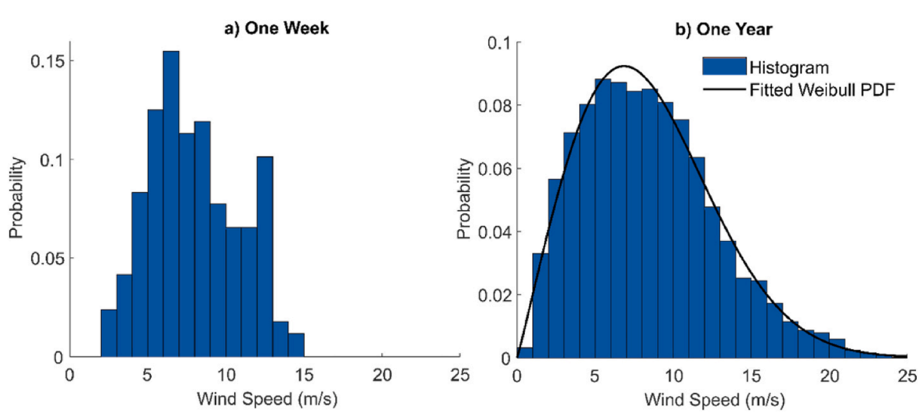

Fig. 4. Probability distribution of one week of wind speed data (a) and one year of wind speed data (b) off the coast of Virginia at 90 m above sea level from DOE BUOY project [42]. The week (a) has a mean wind speed of 8 m/s while the year (b) has a mean wind speed of 8.4 m/s.

Table 1
NREL 5 MW monopile turbine specifications, with site specific information [43–45].

Specification	Value
Rotor diameter	126 m
Blade clearance	24.6 m
Tower height	87.6 m
Depth below water line, above mud	20 m
Depth below mudline	36 m
Diameter, thickness at and below waterline	6 m, 0.027 m
Diameter, thickness at top	3.87, 0.019 m
Rated Power	5 MW
Capacity Factor (site-specific)	0.427
Average Power (site-specific)	2.135 MW

where the average turbine power is 2.135 MW based on the above capacity factor.

2.3. Battery storage options

Potential battery storage options within the wind turbine are compared in Table 2 for LMB, Li-ion, and Lead-acid batteries. The values for the more conventional energy storage battery options of Li-ion and Lead-acid in Table 2 are from Refs. [46,47], and both technologies have been implemented in large-scale storage installations [24,46]. Comparing these two options, Lead-acid is less expensive, but Li-ion has superior performance characteristics, in particular, a much longer cycle life. Space, mass, and life-cycle constraints tend to dominate for long-term installations, which is consistent with Li-ion being the dominant battery option in current large-scale energy storage installations, as of the time of this writing [19].

The LMB storage options include both a published Li–Bi system [35] and an announced Ca–Sb system [39]. The performance specifications for these two systems configured for a large-scale application are listed in Table 2 and discussed below. However, in the absence of a full-scale deployment, LMB performance metrics contain a high degree of uncertainty. The Li–Bi LMB system was tested at lab scale in cells as high as 200 Ah capacity. Note that the Li–Bi system reported in Ref. [35] was not optimized and would be less expensive in a large-scale format. For example, in a large cell the ratio of the thickness to volume of the electrolyte would be significantly reduced. Furthermore, for the large battery comprising hundreds of large-format cells, the metals of the electrodes and the salts of the electrolyte materials would be purchased at bulk market cost, with lower metallurgical-grade purity. In order to estimate cost for a large-scale system composed of Li–Bi LMB, an "optimized" version of the Li–Bi system is used in Table 2 based on estimated manufactured pack cost (with more details on the assumptions in Appendix). For the projected Ca–Sb LMB, the cycle life is from Ref. [36] while the rest of the battery specifications are based on published Ambri estimates [39]. The Ca–Sb system has not yet been commercially installed, but the production cell size is reported to be 800 Ah, which will be aggregated into a 1000 kWh battery.

A comparison of the conventional battery options to the LMB options shows that both Li-ion and Lead-acid have higher roundtrip efficiencies than either LMB option. However, both LMB options have much lower cost than the traditional battery options as well as much higher cycle-life numbers. For integration into a wind turbine that is slated to have 20+ years of operation, low cost and high cycle-life are the driving factors for performance. Additionally, the high energy density of LMB is an advantage when integrating into a structure with finite available space. As such, LMB is a strong candidate for integrated wind energy storage though it requires additional technology development. Details on the how the LMB concept could be integrated are given in the next section.

2.4. Liquid metal battery integration

The proposed integration of LMB into the substructure is shown in Fig. 5 along with a generic cross-sectional design of the LMB. The LMB system would comprise custom-made cells with form factor of either disk (hockey puck-shaped) or prismatic (cereal box-shaped) configuration. Some hundreds of these cells are stacked in the tower substructure so as in aggregate to provide the desired storage capacity, i.e., required voltage and current. However, there is ample space available in the tower substructure since there is approximately 550 m^3 of volume between the waterline and the mudline (Table 1), which is a factor of five more than volume needed for the LMB (details on the battery sizing within the turbine structure are given in Appendix).

Safe operation of the batteries will be critical to their integration into offshore turbine structures. Using properly designed packaging, the LMB system has been demonstrated by Ambri to maintain safe exterior temperature and to keep its core molten by cycling every two days [39]. Joule heating within the battery (the energy loss associated with reductions in round-trip efficiency in Table 2) combined with device insulation and packaging has been found to generate enough heat to maintain the requisite high internal working temperature while ensuring the external temperatures are low [39]. Additional insulation will be added between casing and tower to maintain lower external surface temperatures for the storage system.

The battery stores energy during periods of excess wind power (generation exceeds demand or line size) and then discharges it during periods of low wind power. In particular, a battery management system (BMS) will decide when to store and when to deliver power. The BMS will need its own power electronics, which may be housed in the tower substructure. The space and power requirements of the BMS are expected to very small (relative to that of the turbine) such that they can be neglected with respect to power generation results in the present first-order concept design. However, round-trip efficiency of energy storage and regeneration can be significant and should be considered.

The energy efficiency for a large-scale storage system can be sensitive to the rates of charge and discharge relative to the capacity of the storage system. Given the very large size of the battery relative to the maximum charge or discharge power, the resultant low charge and discharge rates should result in high electrochemical energy efficiency. For the LMB system considered herein, current experimental data suggests there is negligible change in capacity utilization or coulombic efficiency for C rates relevant to the grid LMB in this study, and that the voltage efficiency has a linear dependence on C rate over the same charge/

Table 2
Current and predicted LMB performance compared to other battery types.

Battery type	Specific Energy (Wh/kg)	Energy Density (Wh/L)	Cost ($/kWh)	Cycle Life	Roundtrip Efficiency	Operational Temperature (°C)	Size Built/Tested
Li-ion	150–180	300–350	600-800 (installed)	1500–5000	90%	Ambient (−20°–50°)	129 MWh, Hornsdale Power Reserve, Australia
Lead-acid	35–40	80–90	150-200 (installed)	500-1200	85%	Ambient (−30°–40°)	40 MWh, Chino, California
LMB Li–Bi	113	592	89 (predicted pack cost)	~10,000	70%	~550°	200 Ah (~79 Wh) Li–Bi battery, Cambridge, MA
LMB Ca–Sb (Ambri projections)	–	–	~21 (projected)	~10,000 (projected)	>80% (projected)	~500°	800 Ah (~760 Wh) battery, Marlborough, MA

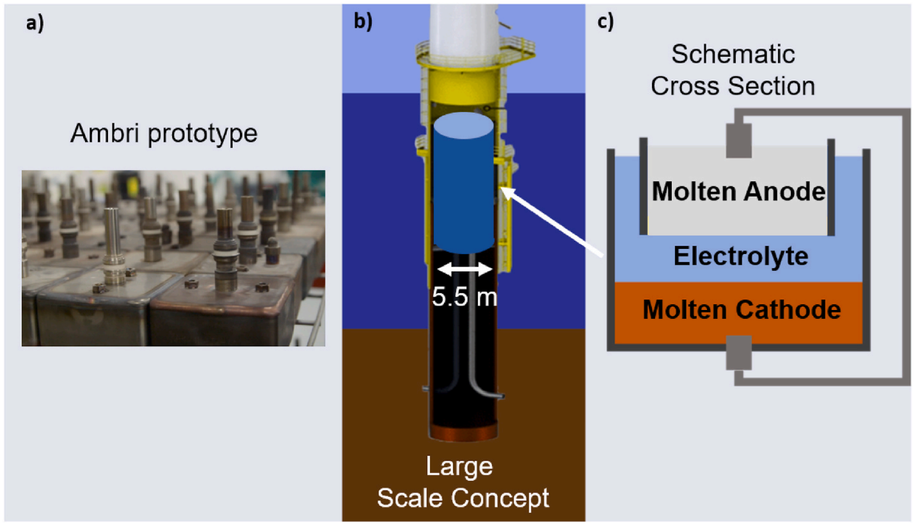

Fig. 5. Liquid metal batteries: a) photo of prototype, b) integrated into offshore wind turbine tower, and c) schematic of active materials.

discharge rates considered [35]. A linear model (Eq. (4)) relating battery charge/discharge efficiency (η) to the battery charge/discharge rate (C) was calculated based on the LMB data provided in Ref. [35], as follows:

$$C = \frac{Rate\ of\ charge/discharge}{Capacity} = \frac{Power}{Energy} \tag{4a}$$

$$\eta = 0.98 - 0.020(hrs) \times C(1/hrs) \tag{4b}$$

In general, the grid-connected LMB system considered in this study will operate at a much lower C rate (<1C) than those previously experimentally evaluated, such that the linear regime is very reasonable approximation. As such, this efficiency model is used for the present study. The energy lost to charge/discharge efficiency for a given power is assumed to all be in the form of Joule heating in the battery (q_{Joule}).

Heat transfer from the battery to the environment must also be considered. Ideally, the heat transfer rates (based on thermal insulation) match the Joule heating rates so that the battery can remain at a nearly constant temperature and there is no additional loss of energy from the system. One may size the thermal insulation to balance this heat generation on average. However, the charge rates (and thus the Joule heating) will vary depending on wind power availability so the heat transfer variations must be considered with respect to both the duty cycle and the operational temperature range associated with a particular LMB chemistry and design. When the Joule heating is high or the battery temperature is close to the peak operating range, active cooling from the much cooler external water may be used. When Joule heating is low or the battery temperature is close to the minimum operating range, heat addition (q_{heater}) can be employed to maintain the operational temperature of the system. Such heat addition is an additional energy loss to the system, so one may define the general energy loss via steady-state heat transfer at any given time as

$$q_{loss} = q_{Joule} + q_{heater} \tag{5}$$

For a 24-h SCAPP system, the average Joule heating of the battery from efficiency losses is 53 kW. This can be used to make a first-order estimate of the thermal insulation system such that average heat loss matches the average Joule heating and minimizes time the heater is needed.

To consider these thermal effects, the key components in the thermal system with a cross-sectional view of the battery within the turbine substructure is shown in Fig. 6. Based on this axisymmetric geometry, the heat lost to the water can be approximated as

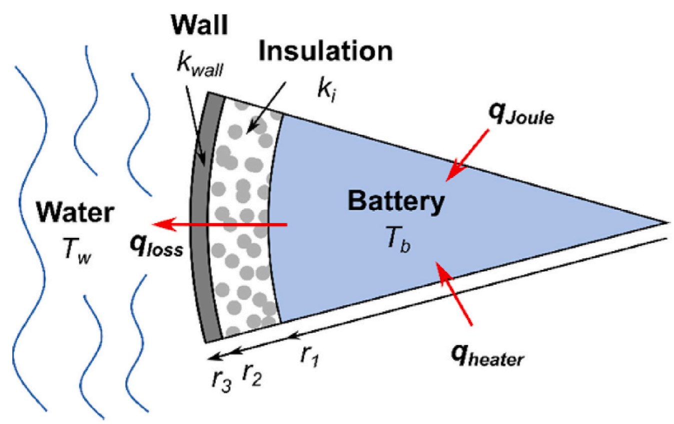

Fig. 6. Cross-sectional schematic of storage system components in thermal circuit.

$$q_{loss} = \frac{T_b - T_w}{\frac{\ln\left(\frac{r_2}{r_1}\right)}{2\pi L k_i} + \frac{\ln\left(\frac{r_3}{r_2}\right)}{2\pi L k_{wall}}} \tag{6a}$$

$$L = \frac{V}{\pi r_1^2} \tag{6b}$$

$$t_i = r_2 - r_1 \tag{6c}$$

where T_b is the LMB operating temperature, T_w is the water temperature, r_3 is the outer substructure radius, r_2 is the inner substructure radius, r_1 is the battery radius, L is the vertical length of the battery within the underwater substructure, k_i is the insulation thermal conductivity, t_{insul} is the insulation thickness, and k_{wall} is the steel wall thermal conductivity. The battery length (L) stems from the volume (V) which is based on the total energy capacity and the LMB energy density. The heat transfer was found to be relatively insensitive to the water free convection, so it was assumed that the outer temperature of the substructure is the same as the water temperature. This temperature was taken as the average water temperature off the coast of Virginia. The design specifications, thermal material characteristics, and system temperatures are given in Table 3 and indicate that an average thermal insulation of 7.6 cm is needed for this system. Given these specifications and assumptions, 53 kW of heat loss is expected, which must be made up by

Table 3
Heat transfer analysis properties and dimensions for 24-h SCAPP system.

Variable	Value
T_b	550 °C (based on Li–Bi, Table 2)
T_w	18 °C [48]
V	86.6 m^3 (based on Li–Bi density, Table 2)
L	3.3 m
r_1, r_2, r_3	2.897 m, 2.973 m, 3.000 m
t_i	7.6 cm
k_{wall}	39.2 W/m-K [49] (Steel at 800 K)
k_i	0.125 W/m-K [49] (alumina-silica blanket at 750 K)

either Joule heating or heat addition to maintain operating temperature of the battery. For a 24 h SCAPP battery system discharging average turbine power (2.14 MW), there is sufficient Joule heating to keep the system warm, but discharging at 0.5 MW requires use of heaters and reduces the one-way efficiency of the battery from 97.6% to 89.4%.

2.5. Levelization and capacity factor results

The levelization and capacity factor are next considered in terms of two independent variables: the maximum electrical connection line size and the storage capacity in terms of hours of average power (SCAPP). Note that the resulting capacity factor is based on power produced to shore. The SCAPP is considered up to 24 h which is enough to ensure significant smoothing and peak reduction. The optimum storage capacity will vary based on turbine size, wind conditions in the chosen location, and the grid valuation of energy as a function of time. Herein, we will employ the baseline 5 MW NREL offshore turbine described in Section 2.2 such that the maximum power delivered is 5 MW when the full 5 MW farm-to-shore electrical connection line is employed.

For the simulations, the charge and discharge strategy is to levelize power production for a given line size. Alternative regeneration strategies could be used based on the system's goal such as minimizing energy loss, reducing hour-to-hour variations in power output [50], or maximizing spot market profit [51]. For the levelization strategy chosen herein, the battery charges when power is produced above the line size limit (until the battery storage is full), and discharges when wind power is below the line size limit (until the battery storage is empty). To reduce the influence of the starting storage level, simulations were run iteratively with the final storage amount carrying over to the starting storage amount until an equilibrium point was reached.

For each timestep in the simulation, any charging or discharging from the battery has an efficiency loss as calculated by Eq. (4). If there is not sufficient Joule heating (q_{Joule}) from the efficiency loss to balance the mean thermal heat loss (q_{loss}), additional energy is used from the battery or reduced from the turbine generation until the necessary 53 kW is met.

The impact of different amounts of battery storage and line sizes on levelization is illustrated in the two examples shown in Fig. 7 for a sample of one week of wind data (sampled from the BUOY wind data as described in Section 2.2). In these figures, the generated wind power shown in grey is bounded by the maximum power output of the turbine of 5 MW, while the delivered power (black line) is bounded by the electrical connection line size. Both are quantified by the left-hand-side vertical axis. In addition, these plots include the battery storage level in orange-dashed line which is quantified by the right-hand-side vertical axis (ranging from 0 to maximum storage). Fig. 7a based on a small reduction in line size (to 4 MW) and 6 h of average wind energy storage capacity. It can be seen that the peak power production is shaved by 1 MW and that the energy storage is often emptied soon after the wind power drops below the rating of the line size. Fig. 7b has a larger reduction in line size (to 2.5 MW) and a larger amount of storage (18 h SCAPP) which results in more frequent storage utilization and a smoother output power profile.

The influence of storage on capacity factor (Eq. (3b)) is considered in Fig. 8 for a range of battery capacities that can provide 0–24 h of SCAPP and for a range of line sized from 2 MW to 5 MW. The capacity factor reflects losses due to curtailment, storage inefficiency (using Eq. (4b)), and heating (q_{heater}). It can be seen that for a fixed amount of storage, reducing the line size, which reduces farm-to-shore connection costs, results in an expected loss in capacity factor. The black line in Fig. 8 denotes 98% of the original wind farm capacity factor, and thus shows how much the line size can be reduced for a given storage capacity without significantly reducing the capacity factor. For example, 98% of

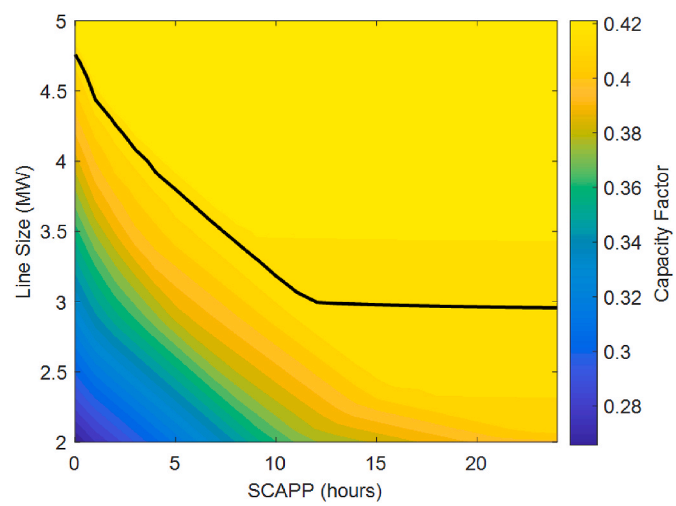

Fig. 8. System capacity factor based on line size and storage time, accounting for losses due to curtailment, inefficiency, and heating. Black line represents 98% of original wind capacity factor.

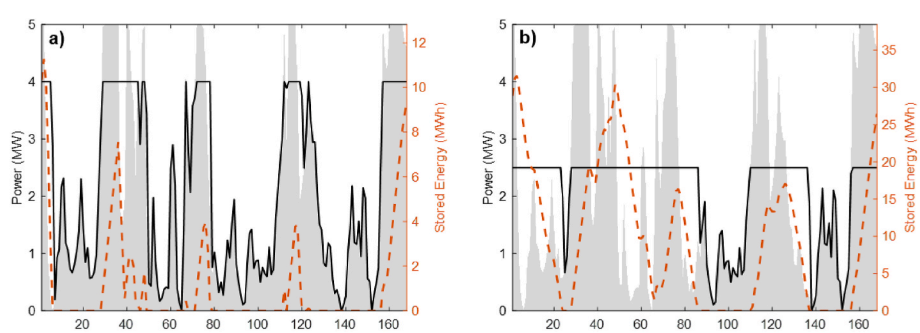

Fig. 7. Two options of line sizes and storage capacities illustrated with zero curtailment for a week of real wind data: a) 4 MW line size and 6 h SCAPP, b) 2.5 MW line size and 18 h SCAPP.

the original capacity factor is maintained with a line size of 4 MW and 4 or more hours of storage, or a line size of 3 MW and 12 or more hours of storage. Reducing line size further requires significantly more storage to retain this capacity factor; thus, one must consider whether the savings associated with reducing line connection outweigh the loss in capacity factor. This compromise will be discussed in the next section. Using battery storage to reduce variations in the wind power output ("smoothing") results in two additional benefits, not quantified here: reduction in penalties for balancing error when wind power output does not meet expected output, and ability to participate in day-ahead market auction [3,25,50].

The average "production efficiency" for each simulated week was calculated as the total energy generated to the grid, divided by the total energy produced by the wind turbine. This is not the storage efficiency, as most energy does not go through the storage system. Instead, this efficiency reflects average losses due to curtailment, storage efficiency, and heating losses, as the system tries to levelized the output power generation. The production efficiency for the 24 h SCAPP system is 96.7%, averaged across all line sizes considered herein, which will be used to simplify the simulations in Section 3.3 case study.

3. Economic analysis

3.1. LCOE and net value of energy

The value of energy produced by a wind turbine can be considered in terms of costs and revenues, and these are generally normalized by the annual energy production in the wind turbine literature as levelized cost of energy (LCOE) and levelized avoided cost of energy (LACE) [52,53]. The baseline LCOE, divided into categories, is pulled from the 2017 Cost of Wind Energy Review for Fixed Bottom Offshore wind turbines [45]. This LCOE includes the annualized costs of a system divided by the annual energy production.

$$LCOE = \frac{(CapEx \times FCR) + OpEx}{AEP} \tag{7}$$

In this expression, CapEx is the total capital expenditures for the system lifetime, FCR is the fixed charge rate which annualizes the capital expenses based on financial considerations, OpEx is the annual operating expenditures, and AEP is the total annual energy production [45].

To value the revenue, LACE annualizes the revenue sources divided by annual energy generation.

$$LACE = \frac{\sum_{i=1}^{Y}(MGP_i \times G_i) + CP}{AEP} \tag{8}$$

$$CP = CV \times CC \times \left(\frac{days}{yr} available\right)$$

In this expression, MGP is marginal generation price (price of energy) in time period i, G is the energy generated in time period i, CP is the capacity payment (the revenue an energy system can earn based on its ability to offset dispatchable resources used to meet peak demand), CV is the capacity value (the annualized cost of a dispatchable resource used to meet peak demand), and CC is the capacity credit (the percentage of installed capacity that can offset reserve requirements during peak demand) [52].

Based on the cost and revenue, the resultant net value (NV) from the system is then the difference

$$NV = LACE - LCOE \tag{9}$$

A system can thus be designed to maximize net value. While the addition of storage will generally increase LCOE, storage may increase LACE such that there is a net improvement in NV.

Information from the 2017 NREL Cost of Wind Energy Review [45] and 2018 Energy Information Administration (EIA) Annual Energy Outlook [53] is used herein for the economic evaluation of turbines with and without storage. For offshore wind turbines in the US, the predicted LCOE is \$124.6/MWh (\$106.2/MWh with tax credits) and LACE is \$47.6/MWh [53]. Even though these estimates result in a net loss (NV < 0), offshore wind farms continue to be built in Europe and are beginning to break ground in the US as well [54]. This can be attributed to additional financial aspects not directly related to engineering design—such as renewable energy credits, different financial assumptions, and government-based and corporate-based decisions to invest in renewable infrastructure. While these factors are important and should be considered in future studies, herein these additional factors are ignored in favor of a focus on engineering design aspects, and only LCOE and LACE will be considered.

Note that LCOE and LACE are used herein due to the current comparable data in the wind turbine literature, but other cost metrics such as COVE [55] and sLCOE [56] may be equally able to consider the potential costs and benefits of adding storage to wind energy.

3.2. Cost and value of energy storage

Quantifying cost of storage depends on the technical specifics of the storage format. The configurations of large-scale LMB and Li-ion storage systems would likely be different when integrated with a wind turbine. Li-ion is typically manufactured in small cells that are then added together in a specific configuration to make modular battery packs [47], while the large-scale configuration of LMB storage is still unknown. Given the unknowns in these potential configurations, LMB and Li-ion storage systems are assumed to be comparable on a kWh basis and costs for both are estimated at the battery pack level.

To determine net cost changes due to the addition of energy storage, BatPaC, a battery cost estimation tool from Argonne National Labs [57,58], was used to estimate the manufactured battery pack costs for a standard Li-ion composition (NMC/Graphite), as well as an LMB composition. The details of this cost analysis and the assumptions used are further specified in the Appendix. The BatPaC results give an average cost of energy capacity for Li-ion NMC/Graphite manufactured battery packs to be \$137/$kWh_{storage}$, where $kWh_{storage}$ is the energy capacity of the battery. The lab-scale Li–Bi system in Ref. [35] was optimized herein for large-scale production and projected to have a manufactured battery pack capacity cost of \$89/$kWh_{storage}$. These costs include estimates for materials, battery management system, and manufacturing cost. These price differences are primarily driven by differences in raw material input prices per $kWh_{storage}$.

To convert battery costs ($CapEx_{battery}$) into total storage costs ($CapEx_{storage}$) into storage system LCOE ($LCOE_{storage}$) comparable to turbine LCOE, we use the following equations.

$$CapEx_{storage}(\$) = CapEx_{battery}\left(\frac{\$}{kWh_{storage}}\right) \times SCAPP(hours) \times P_{avg}(kW) \tag{10a}$$

$$LCOE_{storage}\left(\frac{\$}{MWh_{turbine}}\right) = CapEx_{storage}(\$) \times \frac{FCR\left({}^{1}/_{yr}\right)}{AEP(MWh_{turbine}/yr)} \tag{10b}$$

where the AEP is 18,703 MWh/yr for the turbine, P_{avg} is the average plant power (2.135 MW if no storage), and FCR (real fixed charge rate) is 7% which annualizes the investment over 20 years. This FCR is taken from the 2017 Cost of Wind Energy Review [45] and assumes the storage system would be financed with the wind farm on the same timeframe. This likely underestimates Li-ion costs because of their shorter expected cycle life compared to the lifetime of a wind turbine. Applying Eq. (10) to the three storage capacities considered herein gives the transformed battery costs listed in Table 4.

In general, the batteries will not require additional grid connections or inverters since the battery storage system will be integrated into the wind turbine power generation system (as indicated in Fig. 2) However,

Table 4
LMB Li–Bi and Li-ion battery costs per annual turbine energy generation ($LCOE_{storage}$) for 6, 12, and 24 h of SCAPP.

Battery size (hrs)	Li–Bi ($88.9/$kWh_{storage}$)		Li-ion ($137/$kWh_{storage}$)	
	$CapEx_{storage}$	$LCOE_{storage}$	$CapEx_{storage}$	$LCOE_{storage}$
6	$1,140,000	$4.26	$1,750,000	$6.57
12	$2,280,000	$8.52	$3,510,000	$13.10
24	$4,560,000	$17.00	$7,020,000	$26.30

there will be other cost changes in the system's total LCOE associated with the integration of storage. Storage can be used to levelize power and reduce the electrical connection cost and size from farm-to-shore as shown in Fig. 7. To evaluate the economic impacts of such changes, electrical connection costs are assumed to be proportional to maximum power plus a baseline cost for distance offshore (held fixed at 40 miles) [59], while installation costs are assumed to scale with the cost of the installed parts (turbine, battery storage, electrical, substructure). As such, the battery system increases the turbine installation CapEx costs (due to incorporation of storage) but any associated transmission line reduction decreases the connection installation CapEx costs (due a reduction in connection power rating). Financial costs are assumed to scale with total CapEx (turbine, electrical connection, substructure, BOS, installation, battery storage, installation) and thus can have similar increases and decreases. Herein, OpEx is assumed to remain constant for simplicity, but should be further investigated in later work. The resulting total system LCOE is thus defined by Eq. (11).

$$LCOE_{total} = LCOE_{turbine} + LCOE_{storage} \tag{11}$$

While the above identifies changes in costs due to battery storage, the following considers potential revenue increases due to battery storage. In this economic analysis, the case of 24 h of storage is examined in detail due to its ease of calculation for energy and capacity revenues. The change in value due to the addition of the battery storage is assumed to come primarily from energy arbitrage revenue and capacity credit; the sum of these revenue streams is analyzed via LACE. The baseline energy revenue for the 5 MW wind turbine without storage is calculated by applying the week of wind power utilized in Fig. 7 to each week of 2018 PJM spot market prices (a Mid-Atlantic regional transmission organization) [60]. Utilizing storage, a simple energy arbitrage scheme was implemented using hourly spot price data to estimate revenue. One day (24 h) of SCAPP storage was used to shift average daily wind power output to the times with the highest energy spot market price, with maximum output constrained by line size, as illustrated in Fig. 9. Note that this uses a different storage strategy than that used in Figs. 6 and 7. Additionally, the system was not allowed to charge from the grid, only from generated wind power. An average production efficiency of 96.7% (based on the 24-h SCAPP simulations in Section 2.5) was used (rather than calculating losses due to curtailment, heater loss, and battery efficiency at each time step). This arbitrage scheme was applied for varying line sizes between 2.5 MW and 5 MW to constrain the amount of power that could be produced at once during peak hours. For example, with a 2.5 MW line size, power is produced to the grid at maximum output (2.5 MW) for 19.5 h each day, while a 4 MW line size produced 4 MW of power for 12.25 h.

The next revenue source comes from the capacity payment that wind energy can receive based on its location and which electrical transmission system it feeds into. For example, PJM onshore wind can receive a range of 14.7%–17.6% capacity credit [61], but offshore wind is likely to receive a much higher capacity credit. In this analysis, it is assumed that an offshore wind turbine would receive 33% capacity credit based on how the US EIA calculates LACE for offshore wind turbines [62]. This case study utilizes a capacity price from PJM for the 2021/2022 auction of $140/MW-day [63], which is consistent with past PJM capacity prices

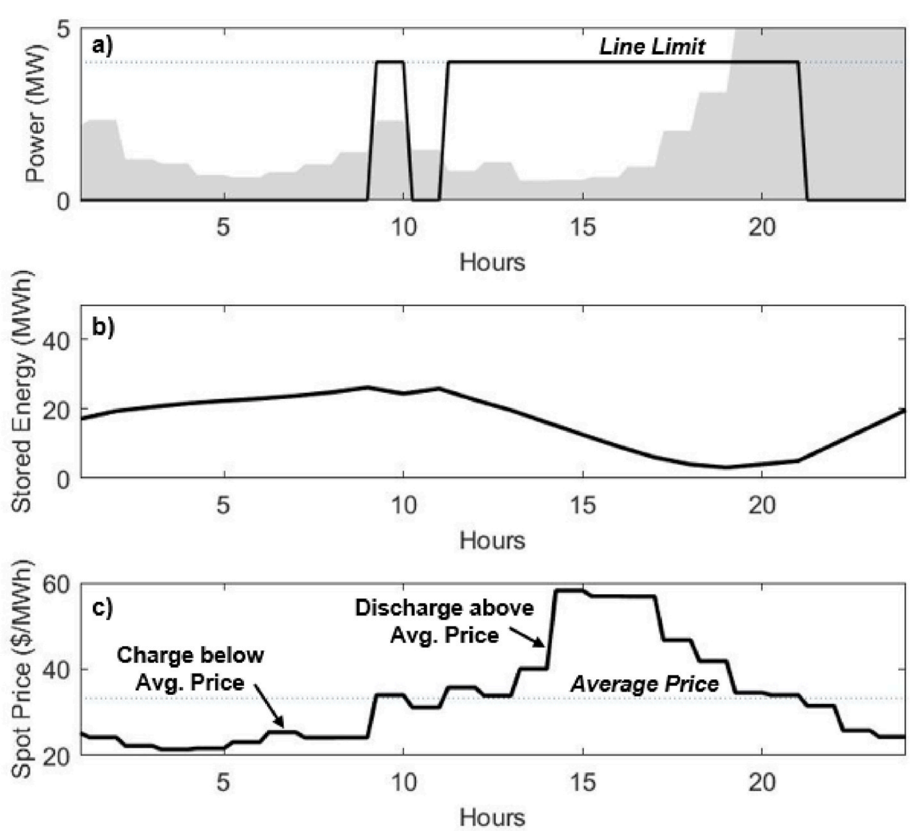

Fig. 9. Energy arbitrage scheme with 24 h of SCAPP and a 4 MW electrical line size depicting a) the wind power generated (grey area) and the electricity generated to shore (black line), b) stored energy over time, and c) spot market price sampled from PJM region.

in the last 10 years [61]. Storage could be optimized to provide maximum capacity payment, limited by line size. Based on results from Ref. [64], 10 h of storage is predicted to earn a capacity credit of over 90%; thus as a first-order estimate, 24 h of storage is assumed to provide sufficient capacity for full credit, limited by line size. A capacity credit of 100% is assumed for all 365 days of the year to determine capacity payment.

In order to compute the changes in LACE with storage, a method is needed that is consistent with the baseline offshore turbine LACE (no storage). If one only combines energy revenue and capacity payments for the baseline wind turbine using Eq. (8) with PJM values for energy and capacity payment, the result computed herein is \$37.5/MWh, which is less than the EIA value of offshore LACE of \$47.6/MWh [53]. This difference can be attributed to additional factors (not included in Eq. (8)) such as the expected increase in natural gas price (and therefore all energy prices) over time and location-dependent price variations. In order to employ current PJM energy and capacity credit prices in this study when evaluating various storage options while still matching LACE values from literature, these additional factors are accounted for by the addition of a PJM scaling factor (f_{site}) for LACE as

$$LACE = \frac{f_{site} \times (Energy\ Revenue + Capacity\ Payment)}{AEP} \tag{12}$$

To match the EIA value for LACE, $f_{site} = 1.27$ is used herein. The introduction of this site factor adds significant uncertainty into the analysis and thus the following results should be considered only as first-order economic estimates to estimate potential economic impact of various design choices. Also, note that other revenue streams associated with storage may also be possible such as forecasted energy balancing, frequency regulation, and other auxiliary services. Currently, such revenue is small and is therefore neglected herein. However, these revenue streams may become increasingly important as renewable energy penetration increases.

3.3. Case study results of economic impact of storage

Based on the above assumptions and methods, the economic impact of storage is considered relative to a baseline offshore wind turbine. This case study assumes a fixed amount of storage capacity of 24 h of SCAPP (equivalent to 51,240 kWh for the 5 MW rated wind turbine) and varies the line size. Lesser amounts of storage will have economic impacts between that of the baseline turbine (with no storage) and the turbine with 24 h of energy storage.

Fig. 10 compares the total LCOE of the original system with a 5 MW electrical connection line to one with 24 h of storage and a 2.5 MW electrical connection line size. While the battery storage does increase the overall system cost, it also allows for reductions in cost in some areas such that the net cost increase is less than the total cost of the batteries.

Next, we consider the revenue aspects for a range of line sizes using PJM 2018 data. As shown in Table 5, there is net savings in the electrical infrastructure associated with reducing the line size (which partially offsets the cost of the battery as noted in Fig. 10). The table also shows that the baseline wind turbine generates \$32.88/MWh in energy revenue (using units as in Eq. (7)), while applying energy arbitrage (with 24 h of storage) resulted in a maximum annual increase in average spot price revenue of 31% over the baseline wind turbine profile. The baseline wind turbine without storage generates \$4.51/MWh (using units as in Eq. (8)) in capacity payment revenue. The breakeven cost is the maximum battery cost at which the economic benefits associated with storage (due to the combination of energy revenue and capacity payment revenue) outweigh the costs. In Table 5, the breakeven manufactured battery pack cost in \$/kWh$_{storage}$ was found by iteratively seeking a battery cost such that the change in LACE and change in LCOE were equal. Thus any battery cost lower than the breakeven cost would reflect a net addition of value to the system, whereas battery costs higher than the breakeven indicate a net reduction of value for integration in this 5 MW offshore wind turbine.

If one now considers a specific battery technology with identified cost per capacity, the likelihood of meeting the breakeven requirements of Table 5 can be determined. The change in net value was calculated (compared to a baseline no storage wind turbine) as shown in Fig. 11 for Li–Bi storage and in Fig. 12 for a variety of storage options. Recall that the integrated storage system is based on a fixed capacity of 24 h of SCAPP. In Fig. 11, the change in LACE and LCOE for the current estimates of LMB storage start as a net loss for the smallest line size since the increase in revenue from storage does not outweigh the battery costs. However, as the line size increases, the increased value becomes greater than the increased cost, resulting in a positive change in net value (the difference between the blue and yellow lines, which is also indicated by the orange line). This indicates that adding 24 h of battery storage, with

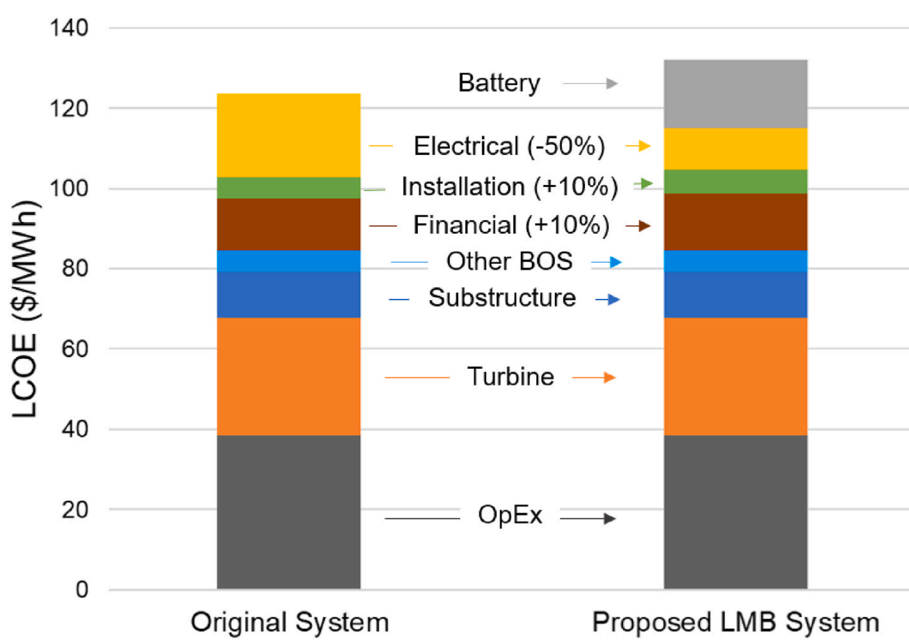

Fig. 10. LCOE effect of switching from Original System with 5 MW line size to Proposed LMB System with 2.5 MW line size and 24 h of SCAPP.

Table 5
Changes with different potential line sizes for a turbine with 24 h of SCAPP (irrespective of storage technology as battery costs are not included).

Line Size	5	5	4.5	4	3.5	3	2.5
SCAPP (hours)	0 h	24 h	24 h	24 h	24 h	24 h	24 h
Electrical Infrastructure Cost Reduction	N/A	0%	9%	18%	27%	35%	44%
Energy Revenue ($/MWh)	$32.88	$43.18	$41.65	$40.56	$38.91	$36.8	$34.58
Capacity Revenue ($/MWh)	$4.51	$13.70	$12.30	$10.90	$9.56	$8.20	$6.83
Breakeven Cost ($/kWh$_{storage}$)	N/A	$100.73	$96.57	$94.70	$89.96	$83.22	$75.11

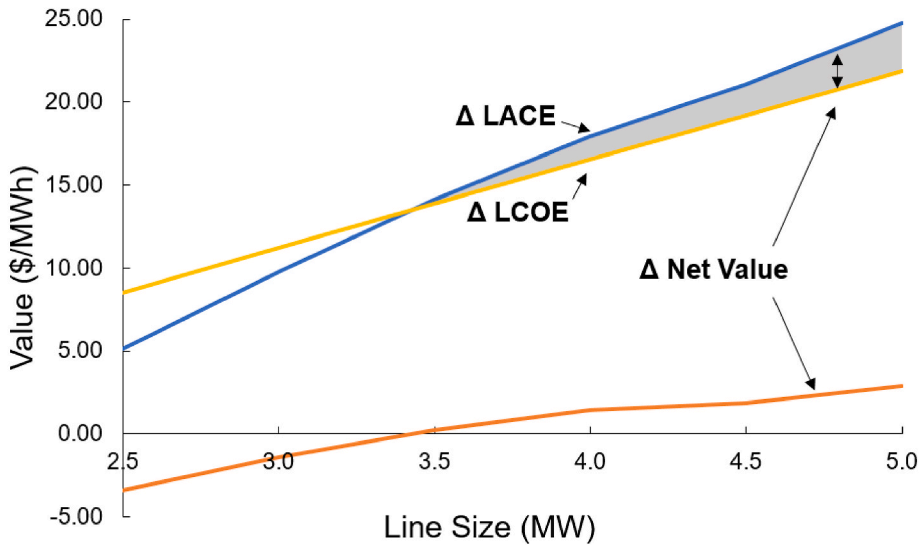

Fig. 11. Change in LACE, LCOE, and Net Value for wind turbine with 24 h integrated Li–Bi storage compared to wind turbine system alone.

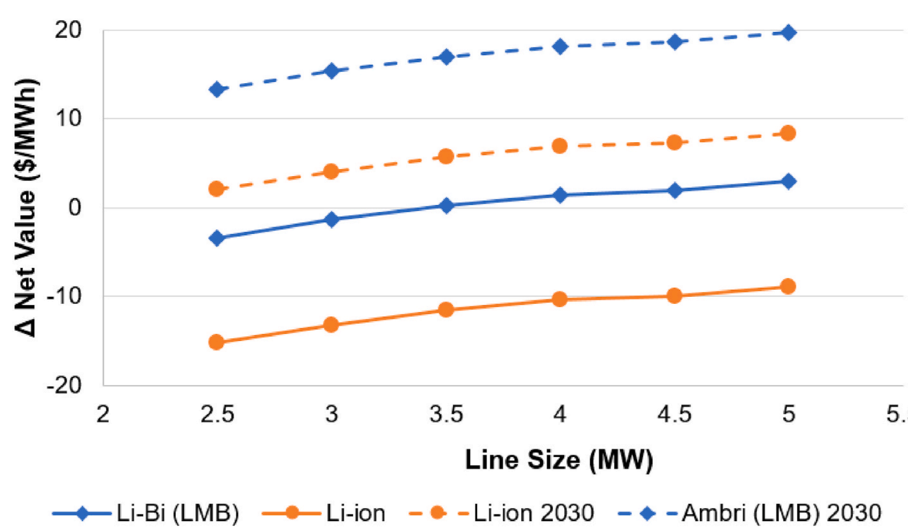

Fig. 12. Change in net value of a turbine with 24 h of storage (compared to baseline wind turbine system with no storage) for current and future Li-ion and LMB predicted costs.

a line size of 3.5 MW or greater, would result in increased profit for the system. Furthermore, it is found that the 5 MW line case gives the maximum increase in NV, indicating that the concept of net cost benefits associated with a reduced line size are never realized for this amount of storage and the given revenue assumptions.

In Fig. 12, the change in net value is plotted for current and future storage costs for both Li-ion and LMB. Costs for storage capacity are based on current predicted LMB (Li–Bi), $89/kWh$_{storage}$; predicted LMB by 2030, $21/kWh$_{storage}$; current Li-ion (NMC/Graphite), $137/kWh$_{storage}$; predicted Li-ion by 2030, $67/kWh$_{storage}$ [30]. All storage types show the same trend of increased value with increased line size, again indicating that the concept of net cost benefits associated with a reduced line size are never realized for this amount of storage for the current case study. In addition, it can be seen that the projected cost decreases in Li-ion and LMB will serve to make energy storage have positive net value in the considered grid application. In particular, the falling cost of Li-ion technology may reach the breakeven cost in the next 10 years. In contrast, the estimated cost of LMB technology is already at the break-even cost and is projected to drop even further in the future, but the LMB technology requires additional development before it will be ready for large-scale commercial applications.

It should be again noted that the present case study results are specific to current PJM data whereas other locations and times would require different scaling factors (Eq. (12)) and so the quantitative results provided herein are for specific conditions and cannot be broadly employed for other locations and future times. However, one may expect that the net value will rise as renewable energy penetration rises since power fluctuations will be stronger and there will be increased value placed on smoothing power output. Additionally, markets with higher capacity prices or more variable energy spot pricing may see additional benefits than demonstrated herein.

4. Summary

To address the resulting mismatches between generation and grid demand and to increase the value of wind energy, long-duration low-cost energy storage is needed as renewables increase shares on the electrical grid. LMB has a potentially very low energy cost and good performance (high efficiency, high cycle life, etc.) and thus may be a good fit for use with wind energy. To investigate a co-located system, the battery capacity is quantified relative to the average plant power rather than the battery rated power. Such a change in perspective is important for an integrated system with energy storage and generation.

A concept is proposed to place the battery within the substructure of offshore wind turbines. By co-locating, simulations indicate that the line size can be reduced to 4 MW with about 4 h of storage, and reduced to 3 MW with about 12 h of storage. Smoothing the wind power output provides additional benefits which could include increased participation in day-ahead market auctions (recommended for future study).

As a case study, 24 h of storage with variable electrical line sizes to shore was analyzed. Reductions in cost due to decreased line sizes, combined with synergistic benefits of co-locating storage and wind energy, results in the total LCOE for a turbine + storage system to be less than the sum of both individual system costs. However, while reducing the line size helps offset the cost of adding batteries, greater value is added to the system in the form of energy and capacity revenue from maintaining high line size, as seen in Fig. 11. Applying energy arbitrage (with 24 h of storage) resulted in a maximum increase in energy revenue of 31% over baseline wind generation. Adding Li–Bi batteries (one optimized form of LMB) to the offshore wind turbine system is predicted to result in a net increase in net value. Breakeven costs are high enough that current LMB technology (Li–Bi) is expected to be profitable and future Li-ion technology is expected to be profitable by 2030, if not sooner.

The present engineering analysis is limited based on current knowledge of liquid metal batteries. The LMB technology is still being developed and changes to the cost and performance estimates are expected in the near future. This simple analysis did not model full battery operation (as in Ref. [18]), consider battery lifetime with a wind-based duty cycle, or investigate the potential increased maintenance for battery integration, and these are recommended for future investigation.

There are also limitations with respect to the economic analysis. The potential cost savings from reducing electrical line size should be further investigated with a more complete electrical system model with a large-scale wind farm. Along these lines, integration and installation aspects for LMB storage with a *floating* wind turbine should be considered, since the weight of the battery may positively help offset cost of ballast weight and the line cost savings are expected to be even larger (as compared to the present fixed-bottom turbine). Furthermore, the economic analysis would also benefit from the application of a detailed energy arbitrage scheme with the policy and temporal constraints of practical energy markets. In addition, the economic analysis is based on the current electrical market, but this market is expected to significantly change with increased renewable penetration in the near future. Based on the above, LMB integration into a wind turbine is highly promising but more work, including an experimental prototype demonstration, is needed to assess its quantitative impact on its net value.

Finally, the environmental impact of integrating a battery storage system into an offshore wind turbine is also of importance. While the footprint of the wind turbines are not expected to change, there may be an increased surface temperature from the LMB system or reduced electrical line sizes, which may affect the local environment. Most importantly, the reduction in carbon emissions from integrating wind turbines with battery storage into the grid could also be quantified and valued.

Credit author statement

Juliet Simpson: Conceptualization, Methodology, Software, Formal analysis, Data curation, Writing – original draft, Visualization, Garrett Hanrahan: Conceptualization, Writing – review & editing, Visualization, Eric Loth: Conceptualization, Methodology, Writing – review & editing, Project administration, Gary Koenig: Conceptualization, Methodology, Writing – review & editing, Donald Sadoway: Conceptualization, Writing – review & editing

Declaration of competing interest

Dr. Donald R. Sadoway is a founder and board member of Ambri, a company commercializing the Liquid Metal Battery. None of the other authors have any conflicts of interest to declare.

Acknowledgments

This work was supported in part by a Sustainability Research Development Grant sponsored by the University of Virginia Committee on Sustainability, and the National Science Foundation Graduate Research Fellowship Program under Grant No. 1842490. Any opinions, findings, and conclusions or recommendations expressed in this material are those of the authors and do not necessarily reflect the views of the National Science Foundation.

The authors would like to acknowledge the help and guidance of Lee Jay Fingersh at the National Renewable Energy Laboratory, Manussawee Sukunta at the Energy Information Administration, and David Bradwell at Ambri.

Appendix A

Specifications of the proposed LMB system based on the optimized Li–Bi chemistry are given in Table A.1. The storage time is based on hours of storage at average power, 2.135 MW. The dimensions are based on the expected interior diameter of the monopile tower substructure (using specifications given in Table 3) and demonstrate that the battery system would take up a small fraction of that space. The battery cost is based on the total manufactured battery pack cost estimated in Table A.2.

Table A.1
LMB Specifications for use in monopile wind turbine, running at average power output, based on reported numbers from Ref. [35] (assuming optimized battery costs) and assumed space available in monopile.

Storage Time (h)	Energy Stored ($MWh_{storage}$)	Mass (Mg)	Volume (m^3)	Height (m)	Battery Cost ($">$)
6	12.81	113.4	21.64	0.82	$1,139,321
12	25.62	226.7	43.28	1.64	$2,278,643
24	51.24	453.5	86.55	3.28	$4,557,286

Table A.2
Battery costs ($/kWh$_{storage}$) based on Li-ion costs from BatPaC and corresponding costs for LMB from Ning et al. [35], optimized Li–Bi, and Ambri

Battery Type	Li-Ion	LMB (Ning)	LMB (opt)	LMB (Ambri)
Chemistry	NMC/Graphite	Li–Bi	Li–Bi	Ca–Sb
Status	*Realized*	*Realized*	*Projected*	*Projected*
Electrode	$42.28	$154.00	$19.41	$17.00
Carbon and Binders	$2.27	$0.00	NA	TBD
Positive Current Collector	$2.08	$2.08	$2.08	TBD
Negative Current Collector	$8.70	$4.35	$4.35	TBD
Separators	$13.56	$0.00	NA	TBD
Electrolyte	$9.45	$66.00	$15.63	$4.00
Cell Hardware	$3.92	$3.92	$3.92	TBD
Module Hardware	$14.07	$14.07	$14.07	TBD
Battery Jacket	$9.87	$4.94	$4.94	TBD
Battery Management System	$11.33	$11.33	$11.33	TBD
Thermal Management System	$0.70	$1.00	$1.00	TBD
Battery Pack Total	$118.24	$261.69	$76.73	TBD
Battery Pack Manufactured Total	$137.06	$303.35	$88.94	TBD

The battery modeling tool BatPaC, developed by Argonne National Lab [57,58], was used extensively to estimate battery costs in this work. The Cost Breakdown Analysis from this tool provided the Li-ion costs for nickel-manganese-cobalt (NMC)/Graphite type batteries in Table A.2 (column 1). Then manufactured battery pack cost for variations on LMB storage were then calculated based on known specifications for different systems, as well as assumptions based on the original BatPaC numbers. The LMB (Ning) column is based on battery specifications found in Ref. [35] for a lab-scale battery; thus, the material costs and quantities are not optimized for full-scale production. The LMB (opt) column attempts to optimize the values from Ref. [35] to reflect the costs of full-scale production by reducing the amount of electrolyte used and switching to market pricing for materials [65, 66]. Finally, LMB (Ambri) is based on the material costs provided by LMB manufacturer, Ambri, and thus reflects the expected future costs of LMB. The assumptions used for each battery component are given in Table A.3 where many components are directly based on the Li-ion costs and the final manufactured cost is based on a scale factor of 1.16 up from the battery pack total (based on the same scaling with Li-ion).

Table A.3
Assumptions used for battery cost components costs for LMB from Ning et al. [35], optimized Li–Bi, and Ambri based on Li-ion BatPaC reference

Battery Type	LMB (Ning)	LMB (opt)	LMB (Ambri)
Electrode	Given	Market prices ($10.78/kg and $100/kg)	Given
Carbon and Binders	N/a	N/a	
Positive Current Collector	=	=	
Negative Current Collector	50% reduction	50% reduction	
Separators	N/a	N/a	
Electrolyte	Given	25% reduction, $5/kg	Given
Cell Hardware	=	=	
Module Hardware	=	=	
Battery Jacket	50% reduction	50% reduction	
Battery Management System	=	=	
Thermal Management System	$1/kWh	$1/kWh	
Battery Pack Total	(summation)	(summation)	
Battery Pack Manufactured Total	(Scale factor)	(Scale factor)	

References

[1] Wiser R, Bolinger M. Wind technologies market report. 2017. 2017.

[2] Esteban MD, Diez JJ, López JS, Negro V. Why offshore wind energy? Renew Energy 2011;36:444–50. https://doi.org/10.1016/j.renene.2010.07.009.

[3] Zhao H, Wu Q, Hu S, Xu H, Rasmussen CN. Review of energy storage system for wind power integration support. Appl Energy 2015;137:545–53. https://doi.org/10.1016/j.apenergy.2014.04.103.

[4] Hirth L. The market value of variable renewables. The effect of solar wind power variability on their relative price. Energy Econ 2013;38:218–36. https://doi.org/10.1016/j.eneco.2013.02.004.

[5] Dykes K, Veers P, Lantz E, Holttinen H, Carlson O, Tuohy A, et al. Results of IEA wind TCP workshop on a grand vision iea wind. 2019.

[6] Wiser R, Mills A, Seel J, Levin T, Botterud A. Impacts of variable renewable energy on bulk power system Assets , pricing , and costs. 2017.

[7] Ahlstrom M, Ela E, Riesz J, O'Sullivan J, Hobbs BF, O'Malley M, et al. The evolution of the market. IEEE Power Energy Mag 2015;6:60–6.

[8] Notton G, Nivet ML, Voyant C, Paoli C, Darras C, Motte F, et al. Intermittent and stochastic character of renewable energy sources: consequences, cost of intermittence and benefit of forecasting. Renew Sustain Energy Rev 2018;87: 96–105. https://doi.org/10.1016/j.rser.2018.02.007.

[9] Kyriakopoulos GL, Arabatzis G. Electrical energy storage systems in electricity generation: energy policies, innovative technologies, and regulatory regimes.

Renew Sustain Energy Rev 2016;56:1044–67. https://doi.org/10.1016/j.rser.2015.12.046.
[10] Bludszuweit H, Domínguez-Navarro JA. A probabilistic method for energy storage sizing based on wind power forecast uncertainty. IEEE Trans Power Syst 2011;26:1651–8. https://doi.org/10.1109/TPWRS.2010.2089541.
[11] Teleke S, Baran ME, Bhattacharya S, Huang A. Validation of battery energy storage control for wind farm dispatching. IEEE PES Gen Meet PES 2010;24:725–32. https://doi.org/10.1109/PES.2010.5589640. 2010.
[12] Ding Y, Shao C, Yan J, Song Y, Zhang C, Guo C. Economical flexibility options for integrating fluctuating wind energy in power systems: the case of China. Appl Energy 2018;228:426–36. https://doi.org/10.1016/j.apenergy.2018.06.066.
[13] Haghi E, Fowler M, Raahemifar K. Co-benefit analysis of incentives for energy generation and storage systems; a multi-stakeholder perspective. Int J Hydrogen Energy 2019;44:9643–71. https://doi.org/10.1016/j.ijhydene.2018.08.150.
[14] Shaner MR, Davis SJ, Lewis NS, Caldeira K. Geophysical constraints on the reliability of solar and wind power in the United States. Energy Environ Sci 2018;11:914–25. https://doi.org/10.1039/C7EE03029K.
[15] Bassett K, Carriveau R, Ting DSK. Energy arbitrage and market opportunities for energy storage facilities in Ontario. J Energy Storage 2018;20:478–84. https://doi.org/10.1016/j.est.2018.10.015.
[16] Salles MBC, Huang J, Aziz MJ, Hogan WW. Potential arbitrage revenue of energy storage systems in PJM. Energies 2017;10. https://doi.org/10.3390/en10081100.
[17] Salles MBC, Gadotti TN, Aziz MJ, Hogan WW. Breakeven analysis of energy storage systems in PJM energy markets. In: 2017 6th int. Conf. Renew. Energy res. Appl. ICRERA 2017; 2017. p. 395–400. https://doi.org/10.1109/DISTRA.2017.8191092.
[18] Jafari M, Botterud A, Sakti A. Evaluation of energy- and capacity-market revenues from lithium-ion battery systems for offshore wind using advanced battery models. Appl Energy 2020. https://doi.org/10.1016/j.apenergy.2020.115417.
[19] US Energy Information Administration. U.S. Battery storage market trends. 2018.
[20] Cole W, Frazier AW. Cost projections for utility-scale battery storage. 2019. Golden, CO.
[21] Denholm P, Mai T. Timescales of energy storage needed for reducing renewable energy curtailment. Renew Energy 2019;130:388–99. https://doi.org/10.1016/j.renene.2018.06.079.
[22] Coffey B. Shades of green: wind-battery hybrid system debuts in Ireland. GE Reports. 2018.
[23] Telsa St John J. Batteries may be used for winter backup on Deepwater's 90MW offshore wind farm. Green Tech Media 2017.
[24] Wahlquist C. South Australia's Tesla battery on track to make back a third of cost in a year. Guardian 2018.
[25] Yao DL, Choi SS, Tseng KJ, Lie TT. Determination of short-term power dispatch schedule for a wind farm incorporated with dual-battery energy storage scheme. IEEE Trans Sustain Energy 2012;3:74–84. https://doi.org/10.1109/TSTE.2011.2163092.
[26] Qin C, Innes-Wimsatt E, Loth E. Hydraulic-electric hybrid wind turbines: tower mass saving and energy storage capacity. Renew Energy 2016;99:69–79. https://doi.org/10.1016/j.renene.2016.06.037.
[27] ARPA-E.. Duration addition to electricitY storage (DAYS) overview. 2018.
[28] Hemmati R, Saboori H. Emergence of hybrid energy storage systems in renewable energy and transport applications – a review. Renew Sustain Energy Rev 2016;65:11–23. https://doi.org/10.1016/j.rser.2016.06.029.
[29] Goldie-Scot L. A behind the scenes take on lithium-ion battery prices. 2019. BloombergNEF.
[30] Colthorpe A. BloombergNEF: bullish on cost reductions, in line with others on global battery market forecast. Energy Storage News 2019.
[31] Kong L, Li C, Jiang J, Pecht MG. Li-ion battery fire hazards and safety strategies. Energies 2018;11:1–11. https://doi.org/10.3390/en11092191.
[32] Lu L, Han X, Li J, Hua J, Ouyang M. A review on the key issues for lithium-ion battery management in electric vehicles. J Power Sources 2013;226:272–88. https://doi.org/10.1016/j.jpowsour.2012.10.060.
[33] Mongird K, Fotedar V, Viswanathan V, Koritarov V, Balducci P, Hadjerioua B, et al. Energy storage technology and cost characterization report. 2019.
[34] Yin H, Chung B, Chen F, Ouchi T, Zhao J, Tanaka N, et al. Faradaically selective membrane for liquid metal displacement batteries. Nat Energy 2018;3:127–31. https://doi.org/10.1038/s41560-017-0072-1.
[35] Ning X, Phadke S, Chung B, Yin H, Burke P, Sadoway DR. Self-healing Li-Bi liquid metal battery for grid-scale energy storage. J Power Sources 2015;275:370–6. https://doi.org/10.1016/j.jpowsour.2014.10.173.
[36] Li H, Yin H, Wang K, Cheng S, Jiang K, Sadoway DR. Liquid metal electrodes for energy storage batteries. Adv Energy Mater 2016;6:1–19. https://doi.org/10.1002/aenm.201600483.
[37] Wang K, Jiang K, Chung B, Ouchi T, Burke PJ, Boysen DA, et al. Lithium-antimony-lead liquid metal battery for grid-level energy storage. Nature 2014;514:348–50. https://doi.org/10.1038/nature13700.
[38] Ouchi T, Kim H, Sadoway DR. Multi-element liquid metal battery. US 2019/0089013 A1. 2019.
[39] Ambri. n.d. https://ambri.com/. [Accessed 29 October 2019].
[40] Qu L, Qiao W. Constant power control of DFIG wind turbines with supercapacitor energy storage. IEEE Trans Ind Appl 2011;47:359–67. https://doi.org/10.1109/TIA.2010.2090932.
[41] Fingersh LJ. Wind-battery-hydrogen integration study wind-battery-hydrogen integration study. 2004. Golden, CO.
[42] US Department of Energy. A2e: BUOY Lidar Project. n.d, https://a2e.energy.gov/projects/buoy. [Accessed 31 August 2018].
[43] Jonkman J, Butterfield S, Musial W, Scott G. Definition of a 5-MW reference wind turbine for offshore system development. 2009. https://doi.org/10.2172/947422.
[44] Jonkman J, Butterfield S, Camp T, Nichols J, Azcona J, Martinez a. Offshore code comparison collaboration within IEA wind annex XXIII : phase II results regarding monopile foundation modeling. IEA Eur Offshore Wind Conf 2008;15. doi:NREL/CP-500-42471.
[45] Stehly T, Beiter P, Heimiller D, Scott G, Heimiller D, Scott G. Cost of wind energy review. 2017. 2018.
[46] May GJ, Davidson A, Monahov B. Lead batteries for utility energy storage: a review. J Energy Storage 2018;15:145–57. https://doi.org/10.1016/j.est.2017.11.008.
[47] Zhang C, Wei YL, Cao PF, Lin MC. Energy storage system: current studies on batteries and power condition system. Renew Sustain Energy Rev 2018;82:3091–106. https://doi.org/10.1016/j.rser.2017.10.030.
[48] National Oceanic and Atmospheric Administration. National data buoy center. Station 44014 n.d, https://www.ndbc.noaa.gov/station_page.php?station=44014.
[49] Bergman TL, Lavine AS, Incropera FP, Dewitt DP. Fundamentals of heat and mass transfer. seventh ed. Wiley; 2011.
[50] Li Q, Choi SS, Yuan Y, Yao DL. On the determination of battery energy storage capacity and short-term power dispatch of a wind farm. IEEE Trans Sustain Energy 2011;2:148–58. https://doi.org/10.1109/TSTE.2010.2095434.
[51] Korpaas M, Holen AT, Hildrum R. Operation and sizing of energy storage for wind power plants in a market system. Int J Electr Power Energy Syst 2003;25:599–606. https://doi.org/10.1016/S0142-0615(03)00016-4.
[52] Levelized EIA. Cost of electricity and levelized avoided cost of electricity methodology supplement. 2013.
[53] Levelized EIA. Cost and levelized avoided cost of new generation resources in the annual energy Outlook. 2018. 2018.
[54] Beiter P, Spitsen P, Nunemaker J, Tian T, Musial W, Lantz E, et al. Offshore wind technologies market update. 2017. 2018.
[55] Simpson J, Loth E, Dykes K. Cost of Valued Energy for design of renewable energy systems. Renew Energy 2020;153:290–300. https://doi.org/10.1016/j.renene.2020.01.131.
[56] Ueckerdt F, Hirth L, Luderer G, Edenhofer O. System LCOE: what are the costs of variable renewables? Energy 2013;63:61–75. https://doi.org/10.1016/j.energy.2013.10.072.
[57] Nelson P, Gallagher K, Bloom I, Dees D, Ahmed S. BatPaC: battery manufacturing cost estimation. 2017.
[58] Nelson PA, Bloom KG, I Dees DW. Modeling the performance and cost of lithium-ion batteries for electric-drive vehicles. Argonne, IL: Chemical Sciences and Engineering division, Argonne National Laboratory, ANL; 2011. https://doi.org/10.2172/1027714. 11/32.
[59] Qin C, Saunders G, Loth E. Offshore wind energy storage concept for cost-of-rated-power savings. Appl Energy 2017;201:148–57. https://doi.org/10.1016/j.apenergy.2017.04.077.
[60] PJM Interconnection. Data miner 2. Real-time hourly LMPs. Historical pricing data 2018, mid-atlantic region [n.d].
[61] Byers C, Levin T, Botterud A. Capacity market design and renewable energy: performance incentives, qualifying capacity, and demand curves. Electr J 2018;31:65–74. https://doi.org/10.1016/j.tej.2018.01.006.
[62] Sukunta M. Personal communication. 2019.
[63] 2021/2022 PJM Interconnection Inc. RPM base residual auction results. 2018.
[64] Sioshansi R, Madaeni SH, Denholm P. A dynamic programming approach to estimate the capacity value of energy storage. IEEE Trans Power Syst 2014;29:395–403. https://doi.org/10.1109/TPWRS.2013.2279839.
[65] Eroglu D, Zavadil KR, Gallagher KG. Critical link between materials chemistry and cell-level design for high energy density and low cost lithium-sulfur transportation battery. J Electrochem Soc 2015;162:A982–90. https://doi.org/10.1149/2.0611506jes.
[66] Singerling SA. Bismuth. 2019. https://doi.org/10.1017/CBO9781107415324.004.